

Tuesday Morning, October 20, 2015

Surface Science

Room: 113 - Session SS+AS+EN-TuM

Mechanistic Insight of Surface Reactions: Catalysis, ALD, etc. - I

Moderator: Ludwig Bartels, University of California - Riverside

8:00am **SS+AS+EN-TuM1 Active Sites of Nitrogen-Doped Carbon Materials for Oxygen Reduction Reaction, Takahiro Kondo, D. Guo, R. Shibuya, C. Akiba, S. Saji, J. Nakamura**, University of Tsukuba, Japan

Nitrogen-doped carbon materials have been found to demonstrate high electrocatalytic activity for oxygen reduction reaction (ORR) as the non-metal catalysts but the active site is still under debate. This is due to the complexity of the real catalysts, such as mixing of different type of N and inhomogeneity in both structure and conductance. Here we designed the nitrogen doped graphite (HOPG) model catalysts with different type of N dominance and its concentration to directly clarify the ORR active site. ORR measurements showed that active site was created by pyridinic N (N bonded to two carbon atoms). The ORR active site was ascribed to the carbon atom with Lewis base property created by neighbour pyridinic N based on the investigations of intermediate state of ORR, localized electronic states at carbon next to pyridinic N and CO₂ adsorption property by X-ray photoelectron spectroscopy (XPS), scanning tunneling spectroscopy (STS) and temperature programmed desorption (TPD), respectively. The ORR activity of model catalyst per pyridinic N concentration was then found to be in good agreement with that for real nitrogen-doped graphene catalyst.

8:20am **SS+AS+EN-TuM2 Cerium Oxide-Induced Intercalation of Oxygen on Supported Graphene, Zbynek Novotny**, Pacific Northwest National Laboratory, *F.P. Netzer*, Karl-Franzens University, Austria, *Z. Dohnalek*, Pacific Northwest National Laboratory

Cerium oxide is an important catalytic material known for its ability to store and release oxygen, and as such, it has been used in a range of applications, both as an active catalyst and as a catalyst support. Using scanning tunneling microscopy and Auger electron spectroscopy, we investigated oxygen interactions with CeO_x clusters on a complete graphene monolayer-covered Ru(0001) at elevated temperatures (550 – 700 K). Under oxidizing conditions (~10⁻⁷ Torr of O₂), oxygen intercalation under the graphene layer is observed. Time dependent studies demonstrate that the intercalation starts in the vicinity of the CeO_x clusters and extends until a completely intercalated layer is observed. Atomically resolved images further show that oxygen forms p(2×1) structure underneath the graphene monolayer. Temperature dependent studies yield an apparent kinetic barrier for the intercalation of 0.9 eV. This value correlates well with the theoretically determined value for the reduction of small CeO₂ clusters reported previously. At higher temperatures, the intercalation is followed by a slower etching of the intercalated graphene (apparent barrier of 1.1 eV). The intercalated oxygen can also be released through the CeO_x clusters by annealing in vacuum. In agreement with previous studies, no intercalation is observed on a complete graphene monolayer without CeO_x clusters, even in the presence of a large number of point defects. These studies demonstrate that the easily reducible CeO_x clusters act as intercalation gateways capable of efficiently delivering oxygen underneath the graphene layer.

8:40am **SS+AS+EN-TuM3 Dissociation Dynamics of Energetic Water Molecules on TiO₂(110): Combined Molecular Beam Scattering and Scanning Tunneling Microscopy Study, Z.-T. Wang, Y.-G. Wang, R.T. Mu, Y. Yoon, G.A. Schenter, R. Rousseau, I. Lyubinetzky, Zdenek Dohnalek**, Pacific Northwest National Laboratory

Molecular beam scattering techniques have proven extremely useful in determining the dynamics of energy flow in the course of chemical reactions. We have successfully designed and constructed a unique, state of the art instrument combining a molecular beam scattering source coupled with a low temperature scanning tunneling microscope (STM). The combination of these techniques allows us to follow the same area during adsorption and image surface species as a function of incident energy of reacting molecules. Our first study focuses on reversible water dissociation on Ti rows of TiO₂(110), which leads to the formation of pairs of terminal and bridging hydroxyl species, H₂O ↔ HO_t + HO_b. The results of our measurements show the onset of H₂O dissociation at 0.2-0.3 eV of incident energy, independent of whether the molecules impinge along or across the Ti rows at an incident angle of 60° relative to surface normal. Following the onset, the dissociation probability increases linearly with increasing incident

energy. Ensembles of *ab initio* molecular dynamics (AIMD) simulations at several incident energies reproduce the product distribution seen in the STM. Additionally, these studies show that the dissociation occurs only for the impacts in the vicinity of surface Ti ions with an activation energy of 0.3 eV and that the O-H bond cleavage is accomplished within the time of a single vibration. The AIMD simulations were further used to construct a classical potential energy surface for water/TiO₂(110) interactions and execute non-equilibrium classical MD simulations that closely reproduce the onset and linear energy dependence of the dissociation probabilities.

9:00am **SS+AS+EN-TuM4 Tracking Site-Specific C-C Coupling of Formaldehyde Molecules on Rutile TiO₂(110), Zhenrong Zhang, K. Zhu, Y. Xia**, Baylor University, *M. Tang*, Southern Illinois University Carbondale, *Z.-T. Wang, I. Lyubinetzky*, Pacific Northwest National Laboratory, *Q. Ge*, Southern Illinois University Carbondale, *Z. Dohnalek*, Pacific Northwest National Laboratory, *K. Park*, Baylor University

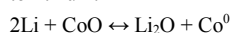
We report the direct visualization of molecular coupling of the smallest aldehyde, formaldehyde, on reduced rutile TiO₂(110) surfaces using scanning tunneling microscope (STM). Images from the same area at viable temperatures (75 ~ 170 K) show that formaldehyde preferably adsorbs to bridging-bonded oxygen vacancy (V_O) defect site. V_O-bound formaldehyde couples with Ti-bound CH₂O form a diolate species, which stays stable at room temperature. In addition, two V_O-bound formaldehyde molecules can couple and form Ti-bound species, which desorbs above ~215 K. This coupling reaction heals both the V_O sites indicating formation and desorption of ethylene. We also directly observed the diffusion of methylene groups to nearby empty V_O sites formed upon dissociation of the C-O bond in V_O-bound formaldehyde, which suggests that the ethylene formation is via coupling of the methylene groups.

9:20am **SS+AS+EN-TuM5 AVS 2014 Gaede-Langmuir Invited Talk: Models for Heterogeneous Catalysts: Complex Materials at the Atomic Level, Hajo Freund***, Fritz Haber Institute of the Max Planck Society, Germany **INVITED**

Our understanding of catalysis, and in particular heterogeneous catalysis, is to a large extent based on the investigation of model systems. The enormous success of metal single crystal model surface chemistry, pioneered by physical chemists, is an outstanding example. Increasing the complexity of the models towards supported nanoparticles, resembling a real disperse metal catalyst, allows one to catch in the model some of the important aspects that cannot be covered by single crystals alone. One of the more important aspects is the support particle interface. We have developed strategies to prepare such model systems based on single crystalline oxide films, which are used as supports for metal, and oxide nanoparticles, which may be studied at the atomic level using the tools developed in surface science. However, those oxide films may also serve as reaction partners themselves, as they are models for SMSI states of metal catalyst. Using such model systems, we are able to study a number of fundamental questions of potential interest, such as reactivity as a function of particle size and structure, influence of support modification, as well as of the environment, i.e. ultra-vacuum or ambient conditions, onto reactivity. The thin oxide film approach allows us to prepare and study amorphous silica as well as 2D-zeolites. Those systems, in spite of their complexity, do lend themselves to theoretical modelling as has been demonstrated.

11:00am **SS+AS+EN-TuM10 The Solid State Li-CoO Conversion Reaction Studied by ARXPS and STM, Ryan Thorpe, S. Rangan**, Rutgers, the State University of New Jersey, *A. Howansky*, Stony Brook University, *R.A. Bartynski*, Rutgers, the State University of New Jersey

Cobalt (II) oxide is a promising electrode material for Li-ion conversion batteries, undergoing the following reversible redox reaction upon exposure to lithium:



In order to characterize the phase progression and morphology of the Li-CoO reaction, epitaxial CoO(100) and (111) films were exposed to lithium in an ultra-high vacuum chamber. The early stages of the reaction were then characterized with scanning tunneling microscopy (STM), while the diffusion of Li into the films and resultant reduction of CoO was quantified using angle-resolved x-ray photoemission spectroscopy (ARXPS). From these measurements, a model of the Li-CoO reaction was constructed for each orientation.

For CoO(111) films, the conversion reaction initiated at step edges and defect sites before proceeding across the surface of the film. STM images of

* Gaede Langmuir Award Winner

CoO(111) after 0.2 ML of Li exposure suggest that the conversion reaction products initially assumed a periodic structure which was in registry with the CoO(111) surface. For larger Li exposures, ARXPS measurements indicated that the reaction proceeded in a layer-by-layer fashion into the bulk, maintaining a planar interface between reacted and unreacted CoO.

The reaction of the CoO(100) surface with 0.1 ML of Li resulted in the formation of 2-3 nm Co metal nanoparticles which decorated the CoO step edges. Upon further lithiation, the conversion reaction proceeded into the film preferentially at step edges. ARXPS measurements suggested that the reaction penetrated deep into the CoO film from these nucleation points before spreading across the rest of the surface. These combined results show the importance of crystallographic orientation in determining the reaction kinetics in a Li-ion battery.

11:20am **SS+AS+EN-TuM11 Imaging Water Adsorption and Dissociation on RuO₂ (110) Surfaces, Rentao Mu, D.C. Cantu, X. Lin, V.A. Glezakou, Z.-T. Wang, I. Lyubinetsky, R. Rousseau, Z. Dohnálek, Pacific Northwest National Laboratory**

Understanding water/solid interactions is a current critical scientific challenge with important implications for a variety of fundamental and applied processes. Here we study the interactions of water with RuO₂, which has a wide range of applications in photocatalytic water splitting, heterogeneous catalysis, electrochemistry and many other energy-related areas. We prepared stoichiometric (*s*-), reduced (*r*-) and oxidized (*o*-) RuO₂(110) surfaces and studied water adsorption, dissociation, and diffusion using time-lapsed scanning tunneling microscopy and density functional theory calculations. On *s*-RuO₂(110) we show that water monomers become mobile above 238 K and form dimers which are immobile below 273 K. More importantly, we find that the mobile water dimers dissociate readily to form Ru-bound H₃O₂ and hydroxyl species (HO_b) on bridging oxygen (O_b) rows. The onset for diffusion of H₃O₂ on *s*-RuO₂(110) is observed at ~273 K, indicating a significantly higher diffusion barrier than that for water monomers. The experimentally determined diffusion barriers are in agreement with those obtained from the DFT calculations. The observed behavior is compared and contrasted with that observed for water on isostructural rutile TiO₂(110) where both molecularly-bound monomers and dimers are in equilibrium with their deprotonated states. In contrast with TiO₂(110), the larger separation of Ru atoms induces the segmentation of water chains at high water coverages. On slightly oxidized *o*-RuO₂(110), water molecules react with oxygen adatoms (O_a's) on Ru rows and form pairs of terminal hydroxyl groups which can reversibly dissociate back to a water molecule and O_a. This process results in the displacement of O_a's along the Ru rows. Along- and across-row diffusion of isolated water molecules is tracked at room temperature on both slightly, and heavily oxidized *o*-RuO₂(110) by following the position of hydroxyl pairs. On *r*-RuO₂(110), we find that water molecules readily dissociate at bridging oxygen vacancies and form bridging hydroxyl groups. The mechanism of along- and across-row diffusion of the bridging hydroxyl protons is also studied at room temperature. The atomically-detailed, quantitative assessment of binding and diffusion of the surface species formed upon water adsorption on RuO₂(110) represent a critical step in achieving fundamental level understanding of the role RuO₂ plays as H₂ and O₂ evolution co-catalysts in photocatalytic water splitting reactions.

11:40am **SS+AS+EN-TuM12 Surface Reaction Kinetics during Low Temperature ALD of Al₂O₃ Studied by Broadband Sum-frequency Generation, Vincent Vandalon, W.M.M. Kessels, Eindhoven University of Technology, Netherlands**

The nonlinear optical technique of broadband sum-frequency generation (BB-SFG) has been used to study the surface reactions during atomic layer deposition (ALD). Vibrational BB-SFG spectroscopy is excellently suited for *in-situ* studies of the surface chemistry governing ALD because of its inherent interface selectivity, submonolayer sensitivity, and short acquisition times. In contrast to BB-SFG, conventional absorption spectroscopy, based on the so called "differential" measurements, monitors only changes on the surface. On the other hand, due to its surface selectivity, BB-SFG reveals information about both *persistent* and *changing* surface groups. Therefore, with this technique, open questions can be addressed such as the origin of the decrease in growth per cycle (GPC) at low temperatures of the ubiquitous process of thermal ALD of Al₂O₃ from Al(CH₃)₃ and H₂O. So far, a complete picture of the surface chemistry explaining the reduced GPC is missing and the exact cause of the limited growth at low temperatures remains unclear.

More particularly, the surface chemistry of thermal ALD Al₂O₃ was followed by monitoring the density of the -CH₃ surface groups. In contrast to ALD at high temperatures, below 200°C it was observed that a significant amount of -CH₃ could not be removed during the water half-cycle. The observed kinetics could not be explained by a thermally-activated first-order reaction with a constant cross section. We investigated the temperature dependence of the reaction kinetics further by measuring the -CH₃ coverage

as a function of precursor and co-reactant exposure at different temperatures. It found that the absolute cross section obtained for the TMA half-cycle was independent of temperature, indicating that the chemisorption of TMA is not a thermally activated process. The behavior during the water half-cycle was found to be more complex showing a strong dependence on temperature; it cannot be described as a reaction simply obeying Arrhenius behavior. This is in line with the more complex behavior predicted by recent DFT work carried out by Shirazi and Elliott [Nanoscale 2015] where a so-called "cooperative" effect was observed leading to a coverage dependent reactivity. The observations presented in this work are direct experimental evidence of such a "cooperative" effect and were only possible due to the inherent surface selectivity of BB-SFG.

12:00pm **SS+AS+EN-TuM13 The Preparation and Redox Properties of Cu/Al₂O₃/ZnO(0001) Model Surfaces, J. Hu, J.J. Huang, H. Zhang, Mingshu Chen, Xiamen University, China**

The Cu/Al₂O₃/ZnO(0001)-Zn ternary model catalysts were prepared and characterized by XPS and LEISS. The Al₂O₃/ZnO was prepared by depositing Al onto the ZnO surface in O₂ atmosphere at 523 K, and Cu/ZnO was prepared by depositing Cu onto ZnO surface at room temperature. It was found that Al₂O₃ grew on the ZnO surface by a layer-by-layer model, while Cu formed two-dimensional islands only at low coverage and three dimensional clusters at high coverage. For Cu/Al₂O₃/ZnO(0001)-Zn, the XPS and LEIS spectra showed that the copper islands were preferred on the interfaces of Al₂O₃/ZnO. Comparing to the Cu/ZnO binary model catalyst, the addition of Al₂O₃ obviously slowed down the reduction of Cu/Al₂O₃/ZnO by H₂. More significantly, the existence of Al₂O₃ in the ternary model catalyst led to an increase of Cu⁺ concentration. The enhancement of Al₂O₃ in Cu/Al₂O₃/ZnO(0001)-Zn for methanol synthesis may originate from that the Al₂O₃ helps to stabilize the surface Cu⁺ which has been proposed as one of the active sites.

Authors Index

Bold page numbers indicate the presenter

— A —

Akiba, C.: SS+AS+EN-TuM1, 1

— B —

Bartynski, R.A.: SS+AS+EN-TuM10, 1

— C —

Cantu, D.C.: SS+AS+EN-TuM11, 2

Chen, M.S.: SS+AS+EN-TuM13, 2

— D —

Dohnalek, Z.: SS+AS+EN-TuM2, 1;
SS+AS+EN-TuM3, 1

Dohnálek, Z.: SS+AS+EN-TuM11, 2;
SS+AS+EN-TuM4, 1

— F —

Freund, H.: SS+AS+EN-TuM5, 1

— G —

Ge, Q.: SS+AS+EN-TuM4, 1

Glezakou, V.A.: SS+AS+EN-TuM11, 2

Guo, D.: SS+AS+EN-TuM1, 1

— H —

Howansky, A.: SS+AS+EN-TuM10, 1

Hu, J.: SS+AS+EN-TuM13, 2

Huang, J.J.: SS+AS+EN-TuM13, 2

— K —

Kessels, W.M.M.: SS+AS+EN-TuM12, 2

Kondo, T.: SS+AS+EN-TuM1, 1

— L —

Lin, X.: SS+AS+EN-TuM11, 2

Lyubinetsky, I.: SS+AS+EN-TuM11, 2;
SS+AS+EN-TuM3, 1; SS+AS+EN-
TuM4, 1

— M —

Mu, R.T.: SS+AS+EN-TuM11, 2;
SS+AS+EN-TuM3, 1

— N —

Nakamura, J.: SS+AS+EN-TuM1, 1

Netzer, F.P.: SS+AS+EN-TuM2, 1

Novotny, Z.: SS+AS+EN-TuM2, 1

— P —

Park, K.: SS+AS+EN-TuM4, 1

— R —

Rangan, S.: SS+AS+EN-TuM10, 1

Rousseau, R.: SS+AS+EN-TuM11, 2;
SS+AS+EN-TuM3, 1

— S —

Saji, S.: SS+AS+EN-TuM1, 1

Schenter, G.A.: SS+AS+EN-TuM3, 1

Shibuya, R.: SS+AS+EN-TuM1, 1

— T —

Tang, M.: SS+AS+EN-TuM4, 1

Thorpe, R.: SS+AS+EN-TuM10, 1

— V —

Vandalon, V.: SS+AS+EN-TuM12, 2

— W —

Wang, Y.-G.: SS+AS+EN-TuM3, 1

Wang, Z.-T.: SS+AS+EN-TuM11, 2;
SS+AS+EN-TuM3, 1; SS+AS+EN-
TuM4, 1

— X —

Xia, Y.: SS+AS+EN-TuM4, 1

— Y —

Yoon, Y.: SS+AS+EN-TuM3, 1

— Z —

Zhang, H.: SS+AS+EN-TuM13, 2

Zhang, Z.: SS+AS+EN-TuM4, 1

Zhu, K.: SS+AS+EN-TuM4, 1